

2D and 3D registration methods for dual-energy contrast-enhanced digital breast tomosynthesis

Kristen C. Lau^{*}, Susan Roth, Andrew D.A. Maidment
University of Pennsylvania, Department of Radiology, 3400 Spruce Street, Philadelphia, PA 19104 USA

ABSTRACT

Contrast-enhanced digital breast tomosynthesis (CE-DBT) uses an iodinated contrast agent to image the three-dimensional breast vasculature. The University of Pennsylvania is conducting a CE-DBT clinical study in patients with known breast cancers. The breast is compressed continuously and imaged at four time points (1 pre-contrast; 3 post-contrast). A hybrid subtraction scheme is proposed. First, dual-energy (DE) images are obtained by a weighted logarithmic subtraction of the high-energy and low-energy image pairs. Then, post-contrast DE images are subtracted from the pre-contrast DE image. This hybrid temporal subtraction of DE images is performed to analyze iodine uptake, but suffers from motion artifacts. Employing image registration further helps to correct for motion, enhancing the evaluation of vascular kinetics. Registration using ANTS (Advanced Normalization Tools) is performed in an iterative manner. Mutual information optimization first corrects large-scale motions. Normalized cross-correlation optimization then iteratively corrects fine-scale misalignment. Two methods have been evaluated: a 2D method using a slice-by-slice approach, and a 3D method using a volumetric approach to account for out-of-plane breast motion. Our results demonstrate that iterative registration qualitatively improves with each iteration (five iterations total). Motion artifacts near the edge of the breast are corrected effectively and structures within the breast (e.g. blood vessels, surgical clip) are better visualized. Statistical and clinical evaluations of registration accuracy in the CE-DBT images are ongoing.

Keywords: contrast-enhanced, dual energy, tomosynthesis, image registration

1. INTRODUCTION

Contrast-enhanced (CE) imaging of the breast is motivated by the observation that angiogenesis occurs in malignant breast lesions [1]. Typically, these new blood vessels have increased permeability and thus the absorption of vascular contrast agents in malignant breast tissue is different than normal breast tissue. As a result, the uptake of intravenous contrast agent can differentiate malignant breast tissue from benign tissue.

Currently, CE magnetic resonance imaging (MRI) is the gold standard for imaging breast cancer perfusion and vasculature. It is used for the characterization of lesions in the diagnosis of breast cancer, and is also recommended as a screening method for women who are at high risk of developing breast cancer. MRI employs a gadolinium contrast agent administered intravenously to highlight morphological features and vascular kinetics. However, MRI does not visualize calcifications, which are early indicators of breast cancer. CE-MRI also suffers from a trade-off between spatial and temporal resolution. Finally, MRI may not be financially feasible as a routine screening method for all women due to high cost.

Several CE x-ray breast imaging modalities have emerged as potential alternatives to CE-MRI, including CE digital mammography (CE-DM), CE digital breast tomosynthesis (CE-DBT), and CE breast computed tomography (CE-BCT) [2]. In comparison to CE-MRI, these imaging modalities have the ability to integrate morphological and vascular kinetic information with high temporal and spatial resolution. Furthermore, they have the potential to become more readily accessible and available since x-ray technology is generally less costly than MRI technology.

DBT is a FDA-approved breast imaging technique for acquiring high-resolution tomographic images of the breast at doses comparable to those used in traditional mammography. CE-DBT uses an intravenous iodinated contrast agent to produce images of the breast vasculature. CE-DBT has the additional advantage of providing tomographic images of the morphology and location of contrast-enhancing lesions. Furthermore, DBT has the ability to acquire

^{*} Kristen.Lau@uphs.upenn.edu, Susan.Roth@uphs.upenn.edu, Andrew.Maidment@uphs.upenn.edu

functional characteristics of breast lesions at high spatial resolution, comparable (or even superior) to that of digital mammography.

Iodine uptake by breast tissue is made more evident by image subtraction. Subtraction removes overlapping anatomical structures that may otherwise occlude the detection and visualization of blood vessels by suppressing variations in the anatomical signal. There are two common types of image subtraction: dual-energy (DE) subtraction, and temporal subtraction [3]. In DE imaging, low-energy (LE) and high-energy (HE) image pairs are acquired. Two distinct x-ray energies are used to differentiate the iodine signal from the soft tissue and to suppress the soft tissue signal. The x-ray energies are chosen so that the k-edge of the contrast agent lies within the range spanned by the LE and HE x-ray spectra. An iodine-enhancement image is created by calculating a weighted difference of the logarithms of the LE and HE images. In DE subtraction, patient motion is minimized because the HE and LE image pairs are acquired either simultaneously or rapidly in sequence. However, DE imaging suffers from inherently lower sensitivity as there is less subject contrast when calculated as the difference of two energies.

In temporal subtraction, images are acquired before and after injection of an iodine contrast agent. The pre-contrast and post-contrast images are then subtracted logarithmically to produce an image of the iodine uptake; the signal from the breast tissue is nulled. However, temporal subtraction is susceptible to patient motion artifacts. Since the total procedure time can be as long as 4-10 minutes, the compressed breast is subject to involuntary motion arising from breathing as well as gross motion of the body over time. Although the breast is held in compression during the study, it has been observed that patients move as a reaction to the contrast injection. This produces subtraction artifacts and thus the quantitative evaluation of iodine uptake is impeded. It also results in a loss of lesion morphology.

We are interested in investigating new methods that eliminate the limitations of DE and temporal subtraction. Specifically, we propose several innovations to reduce the impact of patient motion in CE-DBT. In this paper, we present a hybrid subtraction method involving the temporal subtraction of the dual-energy images. Employing image registration during temporal subtraction further corrects patient motion. These innovations enhance our ability to evaluate the vascular kinetics of breast tumours in CE-DBT imaging. By combining the strengths and minimizing the weaknesses of each subtraction method, we retain the high sensitivity of temporal subtraction while utilizing the resilience to motion of the DE technique.

2. METHODS & MATERIALS

2.1 Image Acquisition

The University of Pennsylvania is conducting a CE-DBT clinical study in which patients with newly diagnosed breast cancers are imaged using a prototype DE Hologic Selenia Dimensions DBT system. The trial is IRB approved and is HIPAA compliant. Currently, 10 patients have been imaged for the study. The goal of this study is to compare CE-DBT to CE-MRI and to quantify the iodine uptake in the breast. Unlike MRI, it is possible to exploit the linear relationship between the attenuation coefficient and the concentration of contrast agent.

The Hologic prototype imaging system consists of an x-ray source with a tungsten target. The angular range of the system is 15° and a single image acquisition lasts 7.3 seconds. A copper filter is used for the HE x-rays (49 kVp) and an aluminum filter is used for the LE x-rays (32 kVp). The mAs is varied to accommodate breasts of different sizes in order to ensure adequate signal to the detector and an acceptable dose to the breast. A total of 22 projections (11 HE, 11 LE) of the breast are acquired in an acquisition sequence. The HE and LE projection images are interleaved. An advantage of this system is its ability to minimize patient motion within a single acquisition because the LE and HE images are obtained virtually simultaneously. Patients are seated and the breast is held in compression for the duration of the exam. Images are obtained at four different time points (1 pre-contrast and 3 post-contrast). A pre-contrast DE image set is acquired to be used as the unenhanced baseline. The iodinated contrast agent, 1 mL/kg of Visipaque-320 (GE Healthcare, Princeton, NJ), is administered intravenously to the patient via a power injector [4]. An intravenous saline flush immediately follows the contrast injection. Post-contrast images are acquired 20 seconds after injection (arterial phase), 1 minute 25 seconds (venous phase), and 3 minutes 25 seconds (late phase). The timing of the post-injection images was determined from previous CE studies [5]. The image acquisition procedure is illustrated in Figure 1.

At each time point, the Hologic prototype produces seven series of images: unprocessed LE and HE projections, unprocessed LE and HE reconstructions, processed LE and HE reconstructions, and a conventional DE

subtraction. The reconstructions are spaced in 2 mm increments. The unprocessed LE and HE reconstructions are reconstructed using simple backprojection; we use these images for our analysis. The processed LE and HE reconstructions and the DE subtraction are intended for clinical assessment by radiologists, but are not clinically evaluated in this paper.

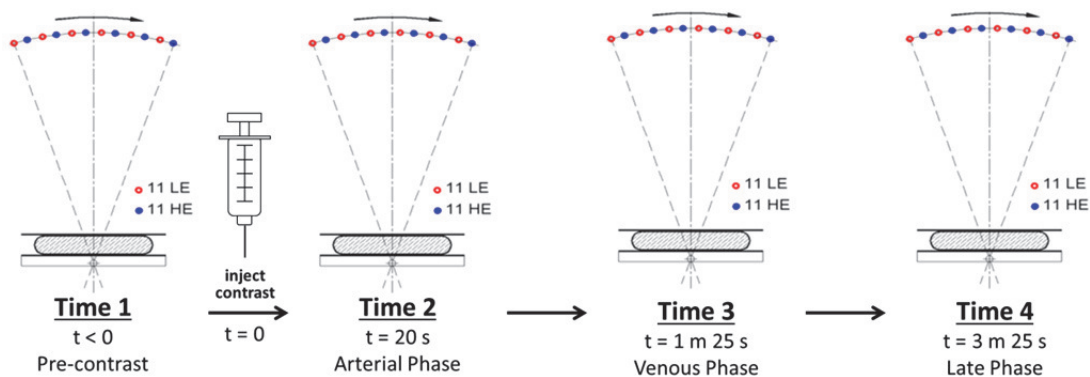


Figure 1. Illustration of the DE CE-DBT clinical trial imaging protocol.

2.2 Hybrid Image Subtraction

In our hybrid subtraction method, we first calculate the DE subtracted images at each time point. This method removes overlapping anatomical structures that may obstruct blood vessels and other enhancing features. In DE subtraction, the DE image is calculated as a weighted logarithmic difference of the LE and HE images,

$$DE = (1 - w) \cdot \ln(HE) - w \cdot \ln(LE) , \quad (1)$$

where w is a weighting factor between 0 and 1. The weighting factor is optimized to null the breast tissue signal in the DE image.

In order to correct for patient motion, we register the post-contrast images to the pre-contrast image. This process is generalized in equation (2). We describe the image registration in detail in Section 2.3.1. Given the unprocessed image I_n , the registered image I'_n is

$$I'_n = I_n \circ \phi_{1,n} \quad \text{for } n = 2, 3, 4 , \quad (2)$$

where n is the post-contrast time point and $\phi_{1,n}$ is the transformation model used to register the n^{th} time point to time 1 (pre-contrast).

Substituting for the HE and LE images into (2), the registered HE and LE images are

$$HE'_n = HE_n \circ \phi_{1,n} \quad \text{for } n = 2, 3, 4 \text{ and} \quad (3)$$

$$LE'_n = LE_n \circ \phi_{1,n} \quad \text{for } n = 2, 3, 4 , \quad (4)$$

where LE'_n and HE'_n denote the registered LE and HE images respectively.

We obtain the post-contrast DE image by substituting equations (3) and (4) into the generalized DE subtraction equation (1). This is given by

$$DE'_n = (1 - w) \cdot \ln(HE'_n) - w \cdot \ln(LE'_n) \quad \text{for } = 2, 3, 4 . \quad (5)$$

The temporal subtraction image ΔDE_n is calculated as the difference between the pre-contrast DE image and the registered post-contrast DE image,

$$\Delta DE_{n,1} = DE'_n - DE_1 . \quad (6)$$

A summary of the subtraction method is given in Figure 2.

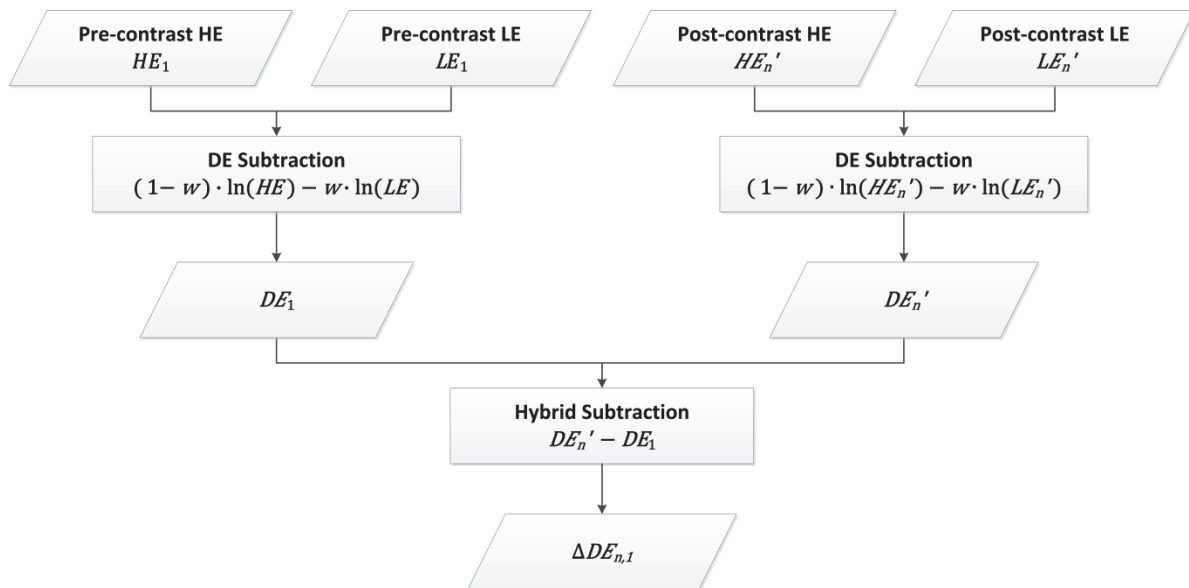


Figure 2. The hybrid image subtraction method. DE images are obtained at each time point via weighted logarithmic subtraction. The DE images are then temporally subtracted between the different time points to produce an iodine-enhanced image.

2.3 Image Registration

2.3.1 Overview

We investigated the registration of the CE-DBT images to correct for patient motion. We used the Advanced Normalization Tools (ANTs) software package developed separately by the Penn Image Computing & Science Lab at the University of Pennsylvania. In this paper, we present this concept in detail and compare the performance of 2D and 3D registration methods. In order to increase computational efficiency, we down-sample the reconstructed images by a factor of 4 in the x and y (in-plane) directions using bilinear interpolation before image registration is performed. The registered images are up-sampled prior to subtraction.

The 2D image registration method is a slice-by-slice approach in which each reconstructed image slice is registered individually. It assumes that patient motion in each slice is confined to that plane and thus is minimal in the z-direction. The post-contrast LE image is first registered to the pre-contrast LE image using ANTs, which generates a deformation map. A diffeomorphic transformation model is used. This single deformation map is applied to both the LE and HE post-contrast reconstructions. The LE image is selected for registration because it is a better anatomical image than the HE image; also, it is less affected by the contrast agent relative to the contrast of the breast tissue. This is summarized in Figure 3.

We also investigate the use of 3D volumetric breast registration because the 2D method does not account for out-of-plane motion that might occur. The results from this 3D volumetric approach are compared with those from the 2D approach. The 3D method also has the potential to improve computational efficiency as the whole 3D volume is registered at one time. In comparison, the 2D approach requires slices to be individually registered and the computational cost is dependent on the number of slices for a particular breast.

2.3.2 Breast Segmentation

The breast skin-line is estimated using the edge detection procedure outlined in Figure 4. Since the anatomical reconstruction by Hologic has well segmented the air region outside the breast, we use the processed Hologic LE reconstruction to obtain a binary mask of the breast. Segmented images are obtained by applying the binary mask to the HE and LE reconstructions (the simple backprojection series). This procedure is applied prior to registration. The results are shown in Figure 6. This reduces the area in an image that needs to be processed, and thus increases the accuracy and efficiency of the registration.

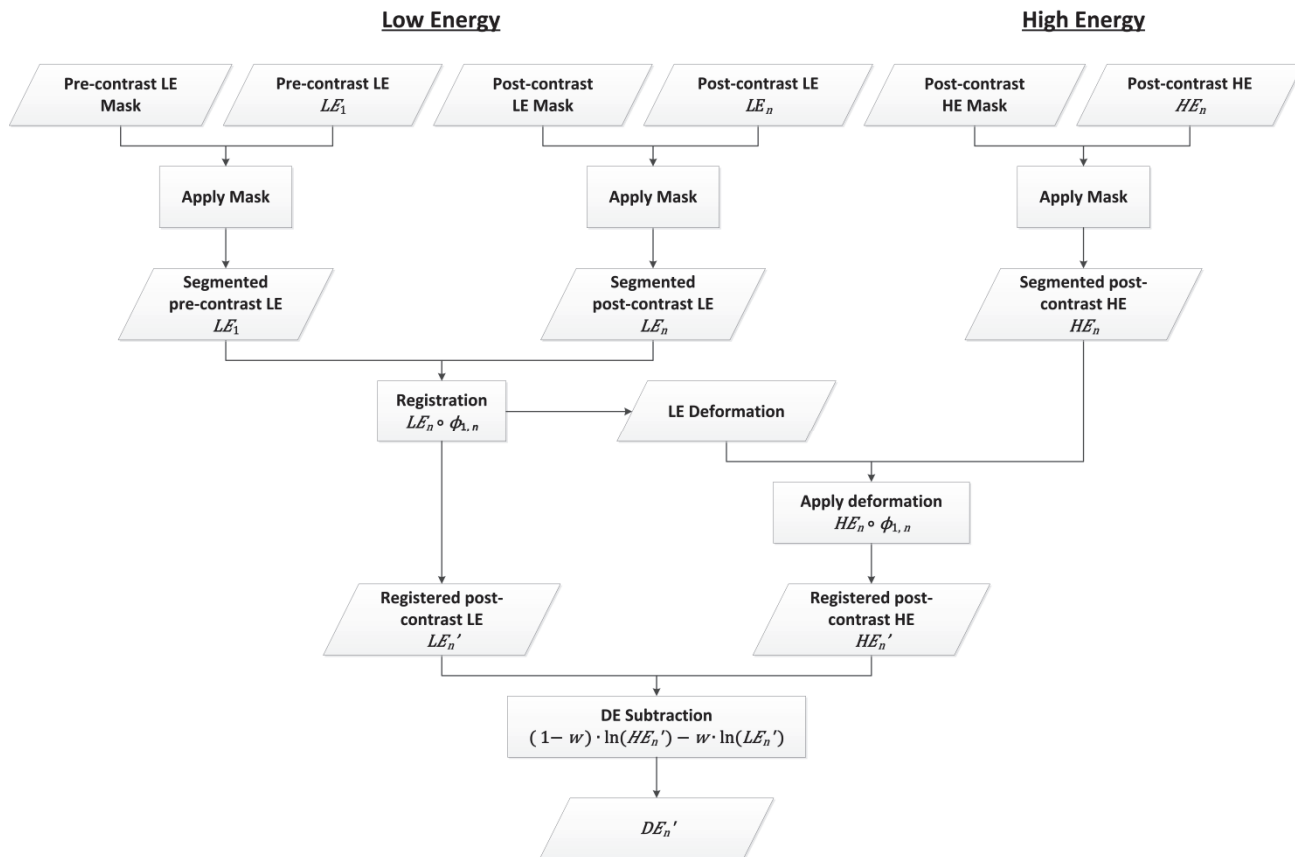


Figure 3. Image registration schema.

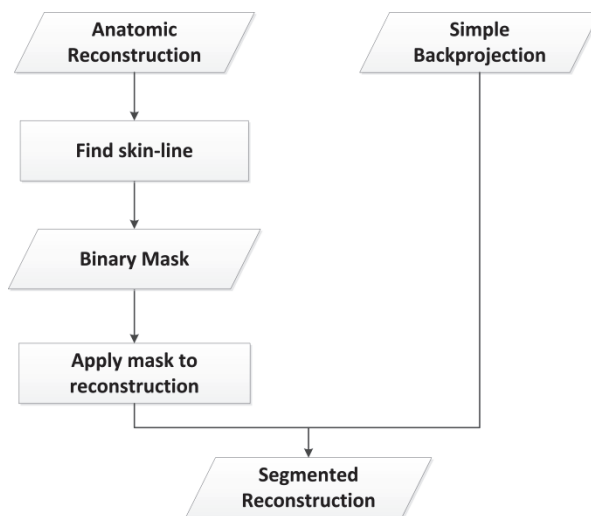


Figure 4. Procedure for segmentation of air.

2.3.3 Iterative Registration Method

We implemented an iterative hybrid registration approach based on the multi-scale deformable registration method for dual-energy x-ray images by Gang *et al.* [6]. This method employs a hybrid algorithm in which a mutual information (MI) optimization is first performed to correct for large-scale motions. A normalized cross-correlation (CC) metric is then used iteratively to correct for misalignment at finer scales. The hybrid approach (as shown in Figure 5) is of interest for this investigation because the mutual information optimization is beneficial in correcting for large-scale breast motion that arises from breathing or during the injection of contrast. Iterative registration using the cross-correlation metric is then used in registering fine-scale misalignment in the breast. In our investigation, we use a total of five iterations for the image registration process.

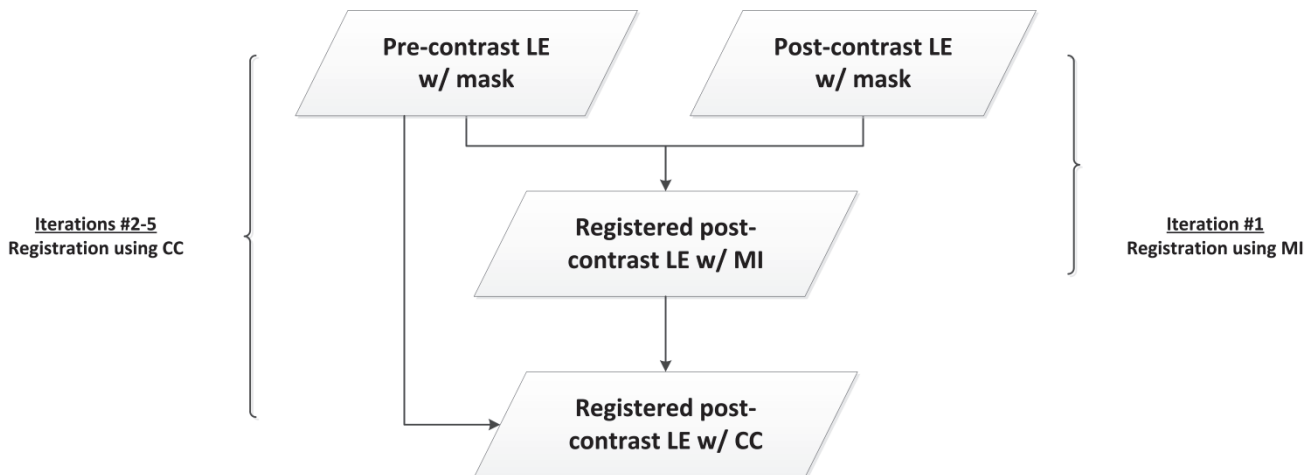


Figure 5. An iterative registration method using both mutual information and cross-correlation optimization.

3. RESULTS & DISCUSSION

3.1 Overview

The 2D registration method was compared to the 3D registration method. The 2D image registration method is a slice-by-slice approach in which each 2D reconstructed image slice is registered individually. The 3D image registration method is a volumetric approach designed to account for out-of-plane motion. We compare the appearance of fiducial markers and anatomical landmarks in the breast, as well as computational efficiency. This procedure was applied to 10 patient cases.

3.2 Breast Segmentation

The segmentation procedure is critical for improving the efficiency of the registration. In the absence of breast segmentation, the registration algorithm will attempt to register the non-uniform region of air outside the breast. An example of the results for our breast segmentation procedure is illustrated in Figure 6.

The region of air outside the breast in the anatomical reconstruction image has been segmented out and is denoted by the uniform black region in Figure 6(a). A binary mask is then created from this image and shown in Figure 6(b). The black region denotes the air and the white region denotes the breast tissue in the binary mask. The binary mask in Figure 6(b) is applied to the LE reconstruction shown in Figure 6(c). The non-uniform grey region in Figure 6(c) represents the non-uniform region of air outside the breast. The resulting segmented image is displayed in Figure 6(d) in inverted grayscale.

Our breast segmentation depends upon Hologic's segmentation algorithm. Although the breast is segmented well in the Hologic reconstructions, the algorithm used may not be best suited for our image processing. A hard edge

boundary between the breast and air results and this may affect registration results. It would be of interest to impose pixel dilation around the boundary in order to avoid having a sharp edge.

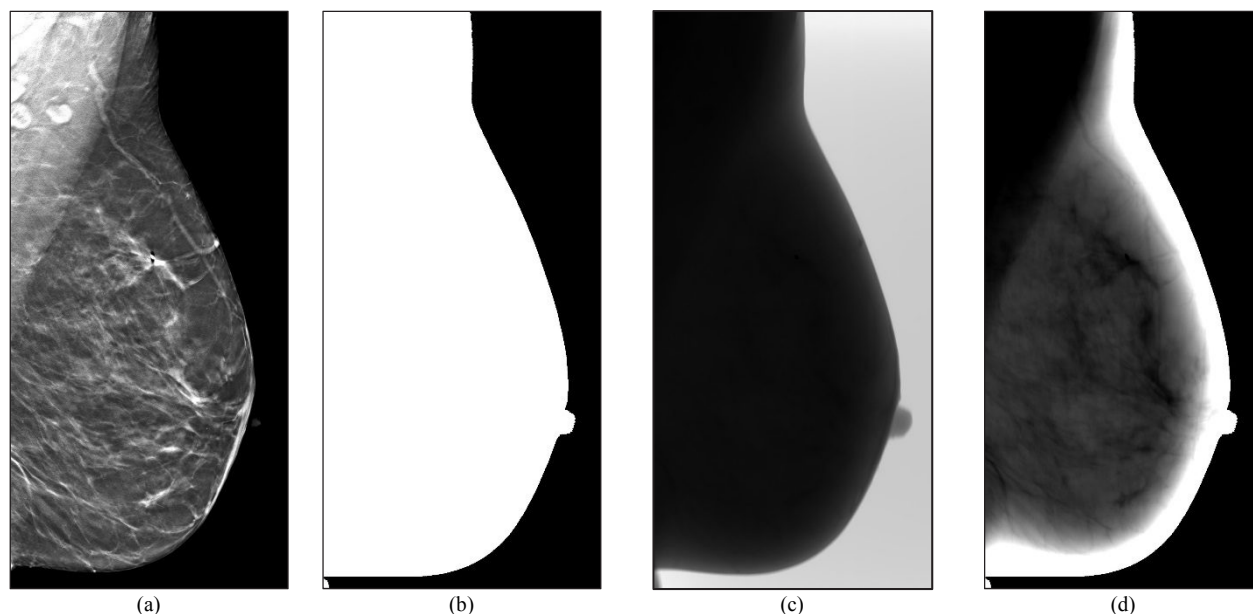


Figure 6. The following series of images are of the same plane in the breast. (a) Anatomical reconstruction of the breast by Hologic. (b) Binary mask obtained from anatomical reconstruction. (c) LE reconstructed prior to segmentation. (d) Segmented LE obtained by applying binary mask.

3.3 Iterative Registration

In this current paper, we evaluate registration accuracy based upon the appearance of natural fiducial markers and obvious anatomic features. Figure 7 illustrates an example of our temporal subtraction results for a particular patient. Magnified views of selected features are shown at each iteration of the registration process. The same planes of the breast are shown using the 2D and 3D registration methods. It is apparent that the motion correction improves with each iteration in both approaches. A total of five iterations are used in this study.

Upon close inspection, we show that the registration results converge by the fourth iteration for the surgical clip in Figure 7. The shadow from the clip is shown to decrease with each subsequent iteration. This holds for both the 2D and 3D registration methods. These results indicate that the registration algorithm can successfully register high contrast objects.

To determine the robustness of the registration algorithm, we examine the registration of low contrast objects such as blood vessels and lymph nodes. These results are also shown in Figure 7. The appearance of blood vessels and lymph nodes are better visualized using the 3D method. The object boundaries are well-defined in comparison to the object boundaries in the 2D method. Motion artifacts near the edge of the breast are also corrected more effectively using the 3D method. This is indicated by the disappearance of a bright band surrounding the edge of the breast.

Currently, we have only identified the surgical clip, lymph nodes, and blood vessels for qualitative evaluation of our registration approaches. However, a limitation of registering low contrast anatomic features is that it depends upon the patient's iodine uptake. Contrast agent uptake could result in poor registration results and object visualization. As a further development in our analysis, it would be beneficial to identify branching points in blood vessels and other natural features in order to have additional natural fiducial markers for quantitative distance measurements.

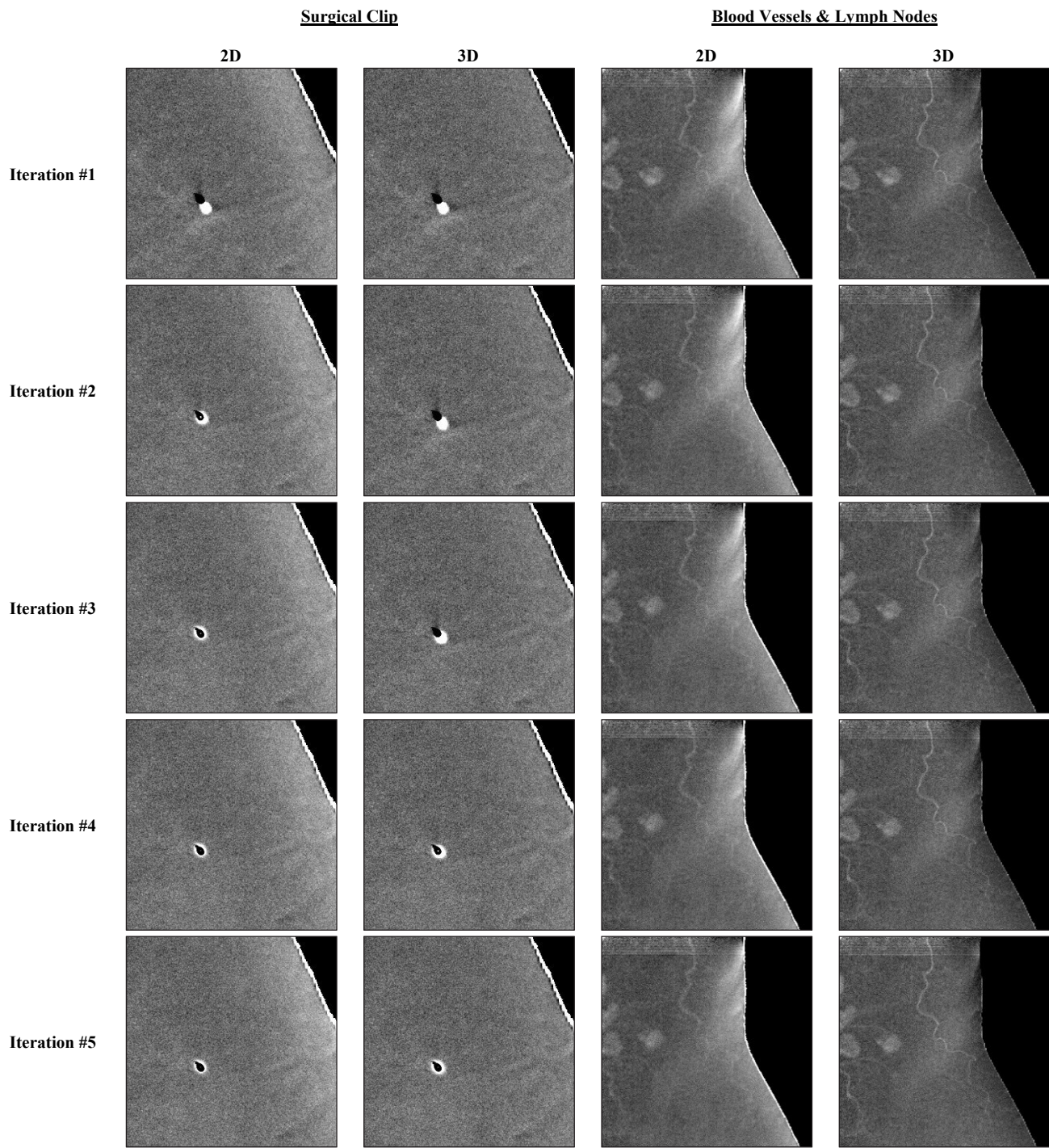


Figure 7. Results of iterative registration using 2D and 3D approaches for a patient. The temporal subtractions are of the same planes of the breast.

3.4 Clinical Evaluation

A preliminary, feature based, clinical evaluation of our results was conducted by trained radiologists. Figure 8 is a complete view of the entire breast used in Figure 7. Identical planes of the breast are displayed, and it can be seen that the motion near the axilla is corrected more successfully using the 3D method. There is still some residual motion at the bottom of the breast that has not been corrected. This is indicated by the bright artifact around the edge of the breast. In addition, blood vessels are better visualized in the 3D result, as indicated by the arrows. The boundaries of the lymph nodes are also better defined in the 3D result.

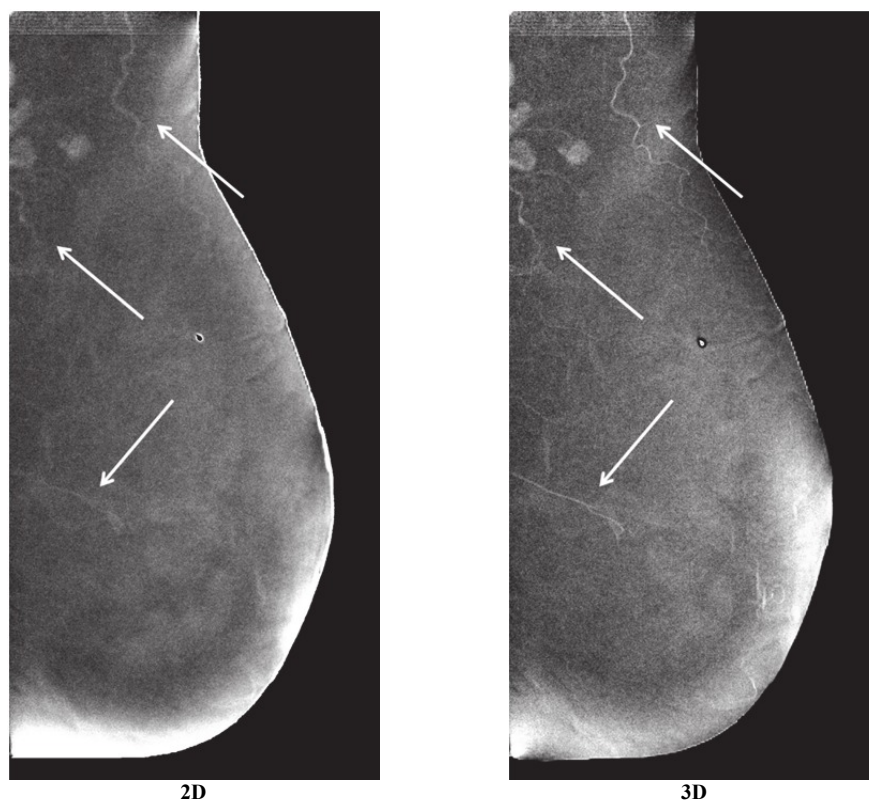


Figure 8. Comparison of 2D and 3D registration methods. The images presented are of the same plane in the breast. A number of blood vessels are indicated by arrows.

Two additional clinical examples of patients with known cancers are shown. Figure 9 is an example of a patient with a small breast size. The main blood vessel runs vertically in the direction of motion of the x-ray tube. DBT is known to have poor slice resolution for objects with a vertical orientation (in the frame of reference of the figure). This blood vessel is strongly visible in each of the reconstructed slices. Our 3D registration method demonstrates that it effectively corrects motion near the edge of the breast for this patient. It also demonstrates that the registration of blood vessels is resistant to directionality. Figure 10 is an example of a patient with a larger breast where the main blood vessel runs horizontally. The lack of artifacts around the blood vessel suggests that 3D registration is well-suited for object localization because sensitivity to motion is greatest in the horizontal direction. Patient motion near the edge of the breast is also corrected more effectively in the 3D method. This is shown in the reduction of the bright artifact surrounding the edge.

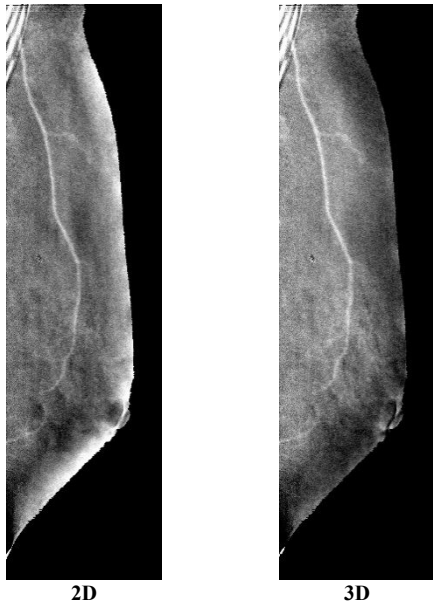


Figure 9. Comparison of 2D and 3D registration methods. The images are of the same plane in the breast. The main blood vessel runs vertically.

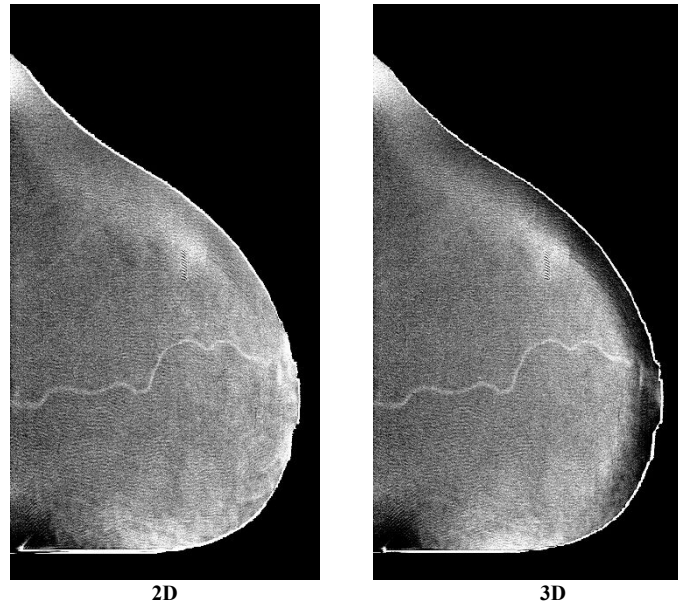


Figure 10. Comparison of 2D and 3D registration methods. The images presented are of the same plane in the breast. In this case, the main blood vessel runs horizontally.

3.5 Computational Efficiency

In comparing the two registration methods for computational efficiency, we only consider the time required to complete the iterative image registration. We assume that the time required to segment the breast, calculate image subtraction, and read/write to disk is constant regardless of registration method. The time required to register the entire breast is dependent upon patient breast size, as this determines the number of breast slices in the reconstruction. The 2D method completes the registration process at an average rate of 2 minutes per slice. The mean breast thickness is 63.7 mm, which corresponds to a mean of 33 reconstructed slices per patient. On average, the 2D registration method requires 60 minutes and the 3D registration method requires 40 minutes. Thus, the computational time for registering the entire breast was reduced by 33% using the 3D method.

While, the 3D registration method was found to be more computationally efficient, the 2D method can be considered more advantageous when registering particular breast slices in real time for clinical evaluation. It also allows for motion in the z-direction to be constrained during registration. In both methods, image registration is performed on the HE and LE reconstructions (not the HE and LE projections).

4. FUTURE WORK

Our study is limited by the number of patients recruited for the study. We have only been able to image 10 women to date and subject recruitment for our study is ongoing. Further investigation of this study involves determining the number of iterations necessary to achieve an acceptable registration and developing a statistical method for evaluating registration effectiveness, such as quantitative distance measures of landmarks in the breast. Additionally, we intend to explore different time combinations for image registration and temporal subtraction. This will allow us to investigate the vascular dynamics between the different post-contrast time points. By identifying the blood vessels in the breast, we can use this segmentation to create a 3D model of breast vasculature and incorporate the vascular tree into a 3D model of the breast. Finally, image evaluation by trained radiologists will provide us with insight on the diagnostic feasibility of DE CE-DBT.

5. CONCLUSION

In our study, we successfully developed a hybrid image subtraction method together with 2D and 3D registration methods for DE CE-DBT images. An approach involving a single deformation for both LE and HE registrations yielded results that were effective. In addition, an iterative registration method using a combination of the single deformation approach and the mutual information and cross-correlation optimization metrics was found to be most effective in registering DE CE-DBT images; it successfully eliminated most of the motion near the edge of the breast. It was also shown to register structures such as blood vessels and surgical clips effectively. Moreover, we were able to implement a successful breast segmentation method that improved the efficacy and computational efficiency of our image registration. In comparison to the 2D method, the 3D registration method proved to be more efficient and reduced computational time by 33%.

ACKNOWLEDGEMENTS

The project described is supported in part by Grant Number UL1RR024134 from the National Center for Research Resources. The content is solely the responsibility of the authors and does not necessarily represent the official views of the National Center for Research Resources or the National Institutes of Health. This work is also supported in part by the Institute for Translational Medicine and Therapeutics' (ITMAT) Transdisciplinary Program in Translational Medicine and Therapeutics. The prototype imaging system is provided to Penn by Hologic (Bedford, MA) under a research agreement. The authors wish to acknowledge the assistance of Jing Zhenxue, Andy Smith, Barry Ren and Chris Ruth from Hologic for technical assistance. The authors would also like to thank Paul Yushkevich for many helpful conversations.

REFERENCES

- [1] N. Weidner, J. P. Semple, W. R. Welch, and J. Folkman, "Tumor Angiogenesis and Metastasis — Correlation in Invasive Breast Carcinoma," *N. Engl. J. Med.* **324**(1), 1–8, Massachusetts Medical Society (1991) [doi:10.1056/NEJM199101033240101].
- [2] A-K. Carton, C. Ullberg, K. Lindman, R. Acciavatti, T. Francke, and A. D. A. Maidment, "Optimization of a dual-energy contrast-enhanced technique for a photon-counting digital breast tomosynthesis system: I. A theoretical model," *Med. Phys.* **37**(11), 5896 (2010) [doi:10.1118/1.3490556].
- [3] A-K. Carton, S. C. Gavenonis, J. a Currivan, E. F. Conant, M. D. Schnall, and A. D. A. Maidment, "Dual-energy contrast-enhanced digital breast tomosynthesis--a feasibility study.," *Br. J. Radiol.* **83**(988), 344–350 (2010) [doi:10.1259/bjr/80279516].
- [4] S. Gavenonis, K. Lau, R. Karunamuni, Y. Zhang, B. Ren, C. Ruth, and A. D. A. Maidment, "Initial Experience with Dual-Energy Contrast-Enhanced Digital Breast Tomosynthesis in the Characterization," *Breast Imaging SE - 5* **7361**, A. A. Maidment, P. Bakic, and S. Gavenonis, Eds., 32–39, Springer Berlin Heidelberg (2012) [doi:10.1007/978-3-642-31271-7_5].
- [5] F. Diekmann, M. Freyer, S. Diekmann, E. M. Fallenberg, T. Fischer, U. Bick, and A. Pöllinger, "Evaluation of contrast-enhanced digital mammography.," *Eur. J. Radiol.* **78**(1), 112–121, Elsevier Ireland Ltd (2011) [doi:10.1016/j.ejrad.2009.10.002].
- [6] G. J. Gang, C. A. Varon, H. Kashani, S. Richard, N. S. Paul, R. Van Metter, J. Yorkston, and J. H. Siewerdsen, "Multiscale deformable registration for dual-energy x-ray imaging," *Med. Phys.* **36**(2), 351 (2009) [doi:10.1118/1.3036981].